Transient heat transfer for helium gas flowing over a horizontal cylinder in a narrow channel

Liu, Qiusheng
Li, Wang
Mitsuishi, Akihiro
Shibahara, Makoto
Fukuda, Katsuya

(Citation)
Experimental Heat Transfer,30(4):341-354

(Issue Date)
2017-03-01

(Resource Type)
journal article

(Version)
Accepted Manuscript

ARTICLE

Transient heat transfer for helium gas flowing over a horizontal cylinder in a narrow channel

Qiusheng LIU[a*], Li Wang[b], Akihiro Mitsuishi[b], Makoto Shibahara[a], and Katsuya Fukuda[a]

[a] *Department of Marine Engineering, Kobe University, 5-1-1, Fukaeminami, Higashinada, Kobe 658-0022, Japan*

[b] *Graduate School of Maritime Sciences, Kobe University, 5-1-1, Fukaeminami, Higashinada, Kobe 658-0022, Japan*

Abstract

Transient forced convection heat transfer due to exponentially increasing heat input to a heater is important as a database for the safety assessment of the transient heat transfer process in a very high temperature gas-cooled reactor (VHTR). Forced convection transient heat transfer for helium gas flowing over a cylinder in a narrow channel was experimentally studied at various periods of exponential increases in heat input. The test heater was mounted horizontally along the center part of a circular test channel with a diameter of 5 mm. The heat generation rates of the heater, $\dot{Q}$, was increased with the exponential function, $\dot{Q} = Q_0 \exp(t/\tau)$. By using a narrow channel, relatively high flow velocity was achieved and experimental data at a high Reynolds number were obtained. According to the results, the surface temperature and the heat flux exponentially increased with time. It was clarified that the heat transfer coefficient approached the quasi-steady-state for a period of more than approximately 1 s, and it reached higher values for a period of less than approximately 1 s. The heat transfer coefficients present high dependence on the flow velocity of the helium gas and the heater diameter. Heat transfer correlations at the quasi-steady state and the transient state were obtained based on the

*Corresponding author. Email: qsliu@maritime.kobe-u.ac.jp

experimental data.

Keywords; Transient heat transfer; helium gas; narrow channel; period; VHTR

1. Introduction

The knowledge of forced convection transient heat transfer phenomenon is important to the design of thermal devices, such as heat exchangers and air heaters. Recently, the heat load has increased, and it requires a compact heat exchanger design with high heat-exchange efficiency. On the other hand, it is important to obtain results regarding the transient forced convection heat transfer affected by the exponential increase of heat input to a heater, for the purpose of building a database for the safety assessment of the transient heat transfer process in a very high temperature gas-cooled reactor (VHTR) [1, 2, 3]. Helium gas is used as coolant in the core of VHTR, and each cylindrical fuel rod is set in circular channels. The coolant flows through the gaps and transports its thermal energy through the fuel rods. This study is focused on the transient thermal hydraulic problem in the core of the VHTR under the reactivity accident condition.

To the best of the authors' knowledge, there are few experimental researches on the transient heat transfer and the narrow channel flow phenomenon for helium gas. Koyama and Asako [4] experimentally investigated heat transfer characteristics of a gas-to-gas counterflow microchannel heat exchanger with a rectangular cross-section of 200 μm in height, 300 μm in width, 20 mm in length, and hydraulic diameter of 240 μm. They concluded that pressure drop is significantly larger than that obtained by conventional correlation. The geometric configuration of a heat exchanger dominates pressure drop characteristics. They also concluded that constant wall temperature model well predicts heat transfer rate of the microchannel heat exchanger. Morini et al. [5] reported experimental results on the Nusselt number for laminar and transitional liquid flows (water and FC-72) through rough stainless-steel micro-tubes of 0.146~0.44 mm inner diameter. They concluded that under laminar conditions, the average Nusselt number approaches the fully developed value for uniformly heated tubes as Reynolds decreases. For higher Reynolds, the region of thermal development increases the average convective heat transfer coefficient, which becomes a function of the Reynolds and Prandtl

number and of the inner diameter-to-heated-length ratio. They also obtained that the average Nusselt steeply increases with Reynolds more than for conventional pipes under transition region. In addition, some researches related to narrow channel flow can be listed as following though the working fluids were liquids, such as water, FC-72 and ethanol. Yang et al. [6] conducted an experimental study of subcooled vertical upward flow boiling of water in a narrow rectangular channel that measures 330 mm in height, 28 mm in width, and 2 mm in height. Piasecka [7] presented some results of FC-72 flow boiling heat transfer in a vertical mini-channel of 1 mm depth, asymmetrically heated by single-sided enhanced foil with various depressions distributed diversely in the area or on the entire surface. Deng et al. [8] systematically investigated the two-phase pressure drop characteristics of reentrant copper micro-channels (D=0.8 mm). They conducted flow boiling tests under a wide range of heat fluxes, exit vapor qualities, and mass fluxes utilizing both water and ethanol.

Liu et al. [1, 9, 10] have reported the experimental data and correlations for parallel flow of helium gas over a horizontal cylinder and a plate. The diameter and the geometric effect of heaters on transient heat transfer were investigated under a wide range of experimental conditions. Meanwhile, the numerical study on transient heat transfer has also been conducted [11]. However, in these previously mentioned studies, the test heater was installed in a circular channel with a relatively large diameter. There are few experimental and analytical works on the transient heat transfer from a heater in a narrow channel with a diameter of several millimeters.

The purpose of this study is to obtain experimental data for the transient forced convection heat transfer of helium gas flowing over a horizontal cylinder in a narrow channel, and to clarify the effects of the narrow channel diameter, velocity, period, and heater diameter on the transient heat transfer phenomenon.

2. Experimental Apparatus and Method

2.1. Schematic diagram of the experimental apparatus

Figure 1 shows the schematic diagram of the experimental apparatus [1]. The experimental apparatus is composed of a gas compressor (2), a flow meter (5), a test section (6), two surge tanks (3, 8), a cooler (7), the heat input control system, and the data measurement and processing system. The vacuum pump was used to degas the loop and the test section. The gas was circulated by compressor, and the fluctuations in gas flow and pressure due to the compressor were eliminated by the surge tanks. Moreover, the gas inside the loop was heated to the desired temperature level by a preheater, and cooled by a cooler, before the gas flowed into the compressor. The flow rate in the test section was measured with a turbine meter, and the pressure was measured with a pressure transducer. The temperature at the exit of the turbine meter and the temperature near the test section heater were measured using K-type thermocouples with a precision of ±1 K. Helium gas was used as the test fluid.

< Figure 1 >

2.2 *Test section and test heater*

Figure 2 shows a vertical cross-sectional view of the test section. The test heater was mounted horizontally along the center part of the circular test channel, with a diameter of 5.0 mm. Four cases were investigated regarding the test heater. Platinum cylinders with diameters of 0.7 mm, 1.0 mm, 1.2 mm, and 2.0 mm were used as test heaters. The test heater was connected to two copper electrodes. Two platinum wires with a diameter of 0.05 mm were spot-welded to the central part of the test heater as potential conductors. The effective lengths of the central parts were 80.53 mm, 84.83 mm, 81.38 mm, and 83.53 mm for the cases of a 0.7 mm in diameter, a 1.0 mm in diameter, a 1.2 mm in diameter, and a 2.0 in diameter heater, respectively.

< Figure 2 >

2.3 *Experimental method and procedure*

The platinum test heater was heated by direct current from a power source. The heat generation rates of the heater were controlled and measured via a heat input control system [12]. The average temperature of the test heater was measured via resistance thermometry using a double bridge circuit, including the test heater as a branch [12, 13]. The test heater was annealed and its electrical resistance versus temperature relation was calibrated in water, and it was washed with a trichloroethylene liquid before being used in the experiment. The heat flux of the heater was calculated using the following equation.

$$q = \frac{d}{4}\dot{Q} - \rho_h c_h \frac{d}{4}\frac{dT_a}{dt}, \tag{1}$$

where ρ_h, c_h, d, and T_a are the density, specific heat, diameter, and average temperature of the test heater, respectively. The test heater surface temperature can be calculated from the unsteady heat conduction equation, presented in following expression, by assuming the surface temperature around the test heater to be uniform.

For the cylindrical test heater, we have,

$$\frac{\partial T}{\partial t} = a\left(\frac{\partial^2 T}{\partial^2 r} + \frac{1}{r}\frac{\partial T}{\partial r}\right) + \frac{\dot{Q}}{\rho c} \tag{2}$$

The boundary conditions are as follows:

$$\left.\frac{\partial T}{\partial r}\right|_{r=0} = 0, \quad -\lambda\left.\frac{\partial T}{\partial r}\right|_{r=R} = q, \quad T_a = \frac{\int_0^R T(2\pi r)dr}{\int_0^R (2\pi r)dr} = \frac{2}{R^2}\int_0^R Tr dr, \tag{3}$$

where $\dot{Q}$ is the internal heat generation rate, T_a is the average temperature of the test heater, q is the heat flux on the surface of test heater, α is thermal diffusivity, and λ is the thermal conductivity.

For the processing of the experimental data, the physical properties of the fluid were calculated based on the following expression for the calculation of film temperature, which was used as the representative temperature.

$$T_f = \frac{T_s + T_l}{2}, \tag{4}$$

where T_s and T_l are the test heater surface temperature and the gas temperature, respectively.

The experiments were carried out according to the following procedure. The test loop was first filled with helium gas after it had been degassed with a vacuum pump. The helium gas was circulated by driving the compressor. The flow rate was gradually lessened from its maximum stream flow. The regulation of the flow rate was carried out by using the by-pass valves of the test section and the by-pass valve of the compressor. After the pressure was confirmed to be stable for each flow velocity in the loop, the electric current was supplied to the test heater, and the heat generation rate was exponentially increased. Then, the test heater's surface temperature and the heat flux were measured throughout the duration of the process.

The uncertainty analysis was performed in our previous research [14]. The maximum uncertainties of heat generation rate, heat flux, and heat transfer coefficient were estimated to be 2.0%, 2.4%, and 4.4%, respectively. The measurement uncertainty analysis was carried out based on the ANSI/ASME performance test codes [15], as shown in Appendix.

3. Experimental Results and Discussion

3.1 *Experimental conditions*

Using platinum test heaters with diameters of 0.7 mm, 1.0 mm, 1.2 mm, and 2.0 mm, the transient heat transfer experimental data were obtained for the heat generation rate periods, which ranged from 40 ms to 20 s, and for a helium gas temperature of 290 K under a pressure of approximately 500 kPa. The flow velocities ranged from 35 to 150 m/s, and the

corresponding Reynolds numbers ranged from 7.2×10^4 to 3.2×10^5. The heat generation rate was exponentially increased according to function, $\dot{Q} = Q_0 \exp(t/\tau)$, where $\dot{Q}$ is the heat generation rate, Q_0 is the initial heat generation rate, t is the time, and τ is the period of the heat generation rate. A lower value or shorter period indicates a higher increasing rate of heat generation.

3.2 *Time-dependence of the heat generation rate, the surface temperature difference, and the heat flux*

Figure 3 shows typical experimental data of the time dependence of the heat generation rate, the surface temperature difference ($\Delta T = T_s - T_l$), and the heat flux at the heat generation rate for increasing periods of 47 ms, 455 ms, and 912 ms, for a flow velocity of 35 m/s (Reynolds number 7.4×10^4). The gas temperature was 290 K. It can be understood that the surface temperature difference and the heat flux increase exponentially as the heat generation rate increases according to the exponential function.

< Figure 3 >

3.3 *Heat transfer coefficient in the transient heat transfer process*

The heat transfer coefficient, h, is defined as follows.

$$h = q/\Delta T \tag{5}$$

Figure 4 shows the heat transfer coefficients versus time for a velocity of 35 m/s, at the period of 912 ms, and gas temperature of 290 K. The heat transfer coefficients approach lower constant values from their higher initial values when the time exceeds approximately 5 times the period ($t/\tau > 5$). It was confirmed that the heat transfer coefficients asymptotically approach values at all periods, velocities, and gas temperatures. These asymptotic values will be used as the transient heat transfer coefficients.

< Figure 4 >

3.4 *Transient heat transfer for various periods of heat generation rate*

Figure 5 shows the relation between the heat transfer coefficient and the period of the heat generation rate, at a gas temperature of 290 K. The heat transfer coefficient, *h*, approaches an asymptotic value for every velocity, when τ exceeds 1 s. In this region, heat is transferred, as well as a usual convective heat through the thermal boundary layer, which was influenced by the helium gas flow. This phenomenon is called quasi-steady-state heat transfer. On the other hand, when the period τ was less than approximately 1 s, h increased as τ decreased. This behavior shows that the heat transfer process is in the unsteady state and the heat transfer in this region has been greatly influenced by the temperature gradient within the thermal boundary layer around the test heater. Especially, in the region of τ less than 200 ms, the thermal boundary layer became very thin; then, the conductive heat transfer near the heater governed the heat transfer process, and the heat transfer coefficient increased greatly within the shorter period in this region. It was clarified that the heat transfer phenomenon was divided into a quasi-steady-state heat transfer and a transient heat transfer on a time boundary of approximately 1 s. The heat transfer coefficient increased with the increase in flow velocity, as shown in Fig. 5.

< Figure 5 >

3.5 *Heat transfer for various diameters of the test heater*

Figure 6 illustrates the heat transfer in a narrow channel for various heater diameters; the flow velocity is 100 m/s, gas temperature is 300 K, and pressure is 500 kPa. As indicated in this figure, the heater diameter significantly affects the heat transfer; the heat transfer coefficient reaches higher values as the heater diameter becomes smaller.

< Figure 6 >

3.6 *Comparison of the experimental data of a 5 mm diameter channel with those for large*

diameter channels

Figure 7 shows the heat transfer coefficients for different channel diameters at a velocity of 35 m/s, and a gas temperature of 290 K. The authors have measured the heat transfer coefficients for the forced convective flow of helium gas over horizontal cylinders using a flow channel with a diameter of 10 mm [16]. As indicated in Fig.7, the values of the heat transfer coefficients in a 5 mm diameter channel are lower than the coefficient values in a 10 mm diameter channel. Figure 7 shows that the heat transfer from the cylinder was affected by the narrow channel.

< Figure 7 >

The authors have reported the heat transfer for a cylinder in a large channel with a diameter of 20 mm in their previous work [10]. The correlation for the quasi-steady-state heat transfer was obtained as $Nu_{st} = 2.2Re^{0.5}Pr^{0.4}$,where $Nu_{st} = h_{st}L/\lambda$, $Re = UL/\nu$; Nu_{st} is the Nusselt number for the quasi-steady-state heat transfer, *Re* is Reynolds number, h_{st} is the quasi-steady-state heat transfer coefficient, and *Pr* is the Prandtl number. The correlation values are shown in Fig.8 for comparison with the data obtained for the channel of 5 mm in diameter. The values of the correlation are approximately 35% higher than those of the narrow 5-mm diameter channel. Based on the results shown in Figs.7 and 8, it was clarified that the narrow channel significantly affected the heat transfer from the cylinder heater. It is considered that the deterioration of heat transfer in a narrow channel is due to the boundary layer developed along the cylinder.

< Figure 8 >

To gain an insight about the boundary layer, the boundary layer thickness along the cylinder was evaluated based on the following equation of the laminar boundary layer theory [17].

$$\delta = 5.0xRe^{-0.5}, \tag{6}$$

where δ is the boundary layer thickness, *x* is length from the edge of the cylinder, and *Re* is

Reynolds number.

Figure 9 shows the boundary layer thickness along the heater at various film temperatures (T_f, Eq.(4)). As it can be observed from Fig.9, the thickness increases with the increase in film temperature. At a position of 100 mm from the leading edge, the boundary layer thickness approaches 2 mm, where the boundary layer comes in contact with the wall of the narrow channel. Compared to the large channel with a diameter of 20 mm, the flow area was considered to be largely occupied by the boundary layer, which then brings the deterioration in the heat transfer.

< Figure 9 >

3.7 *Correlation of quasi-steady state heat transfer and transient heat transfer*

Figure 10 demonstrates the relationship between the Nusselt numbers and the Reynolds numbers of helium gas at the periods ranging from 1.7 s to 17 s. They are shown in the $Nu_{st}/Pr^{0.4}$ versus Re graph. As shown in the figure, the Nusselt number increases linearly with increase in the square root of the Reynolds number. The Nusselt number for the quasi-steady-state heat transfer can be correlated via the following empirical equation.

$$Nu_{st} = 1.62(d/d_0)^{-0.5} Re^{0.5} Pr^{0.4}, \tag{7}$$

where, d is the cylinder diameter, and d_0 is a reference diameter of 1.0 mm.

The empirical correlation of Nusselt number for the cylinder obtained from the experimental data is compared with the previous laminar analytical solution for plate (Eq.(8), [17]) in Fig11. As shown in Fig.11, the Nusselt numbers for the cylinder are larger than those for the plat due to the geometric effect.

$$Nu = 0.664 Re^{0.5} Pr^{1/3} \qquad \text{for plate} \tag{8}$$

As stated in the Introduction, Liu et al. [1] carried out experiments on the transient heat transfer of helium gas for a plate with a width of 4 mm. They obtained an empirical correlation of the ratio of the transient Nusselt number, Nu_{tr}, to the quasi-steady-state Nusselt number, Nu_{st},

using a dimensionless period of τ^*·($\tau^* = \tau U/L$). The present experimental data can also be correlated in this way. As shown in Fig.12, the empirical correlation for a cylinder with a 0.7 mm diameter can be obtained from the following.

$$Nu_{tr} = Nu_{st}(1 + 4.74\tau^{-0.8}), \quad (9)$$

For other cylinders, the coefficient in Eq.(9) is different from the value (i.e. 4.74) for 0.7 mm diameter cylinder. It can be obtained as 13.66, 6.95, and 20.69 for the cylinders with diameters of 1.0 mm, 1.2 mm, and 2.0 mm, respectively. The experimental data agree well with the values obtained via Eq. (9), as shown in Fig.12.

< Figure 10 >

< Figure 11 >

< Figure 12 >

4. Conclusions

The transient heat transfer coefficients for forced convection flow of helium gas over a horizontal cylinder were measured using a narrow test channel, and the following results were obtained.

(1) The heat transfer coefficient was dependent on the gas flow velocity, and largely dependent on the diameter of the test heater.

(2) The transient heat transfer from the cylinder was affected by the size of the channel diameter, particularly as the diameter of the channel was reduced and reached a value of 5 mm.

(3) The deterioration of heat transfer in a narrow channel is considered to be due to the flow area becoming largely occupied by the developed boundary layer.

(4) Heat transfer correlations at the quasi-steady-state and the transient state were obtained based on the experimental data.

Nomenclature

a thermal diffusivity (m^2/s)

c_h specific heat of test heater, J/(kgK)

D diameter of channel, mm

d diameter of cylinder, mm

d_0 reference diameter of 1 mm

h heat transfer coefficient, W/m^2 K

L effective length of heater, m

Nu Nusselt number, hL/λ

Pr Prandtl number

$\dot{Q}$ heat generation rate per unit volume, W/m^3

Q_0 initial heat generation rate per unit volume, W/m^3

q heat flux, W/m^2

R Radius of the cylinder, m

Re Reynolds number, UL/ν

r coordinate along the radial direction of the cylinder, m

T temperature, K

T_a average temperature of the test heater, K

T_l gas temperature, K

ΔT temperature difference between cylinder surface and gas, K

t time, s

U velocity of helium gas, m/s

x length from the edge of the cylinder, m

δ boundary layer thickness, m

ρ_h density of test heater, kg/m^3

λ thermal conductivity of test heater, W/mK

ν kinematic viscosity of helium gas, m^2/s

τ period of heat generation rate or e-fold time, s

Subscript

s surface of test heater

st quasi-steady state

tr transient state

Acknowledgments

This work was supported by the Japan Society for the promotion of Science (JSPS) (Grant-in Aid for Scientific Research (C), KAKENHI, No.15k05829).

Appendix

The measurement uncertainty was estimated based on the ANSI/ASME performance test codes [15]. The maximum uncertainty of heat generation rate can be obtained by Eqs. (A1)-(A3).

$$\frac{B_{\dot{Q}}}{\dot{Q}} = \sqrt{\left(\frac{\partial \dot{Q}}{\partial V}\right)^2 \left(\frac{B_{V_R}}{V}\right)^2 + \left(\frac{\partial \dot{Q}}{\partial V}\right)^2 \left(\frac{B_{V_I}}{V}\right)^2} \tag{A1}$$

$$\frac{S_{\dot{Q}}}{\dot{Q}} = \sqrt{\left(\frac{\partial \dot{Q}}{\partial V}\right)^2 \left(\frac{S_{V_R}}{V}\right)^2 + \left(\frac{\partial \dot{Q}}{\partial V}\right)^2 \left(\frac{S_{V_I}}{V}\right)^2} \tag{A2}$$

$$\frac{U_{RSS,\dot{Q}}}{\dot{Q}} = \sqrt{\left(\frac{B_{\dot{Q}}}{\dot{Q}}\right)^2 + t_{95}\left(\frac{S_{\dot{Q}}}{\dot{Q}}\right)^2} \tag{A3}$$

where, $B_{\dot{Q}}$, $S_{\dot{Q}}$ and t_{95} are the basis of the heat generation rate, the precision index of the heat generation rate, and confidence level, respectively. B_V and S_V are the basis and precision

index of the DC amplifier (Yokogawa, 3131). On the other hand, the maximum uncertainty of the heat flux can be obtained by Eqs. (A4)- (A6).

$$\frac{B_q}{q}=\sqrt{\left(\frac{\partial q}{\partial V}\right)^2\left(\frac{B_V}{V}\right)^2+\left(\frac{\partial q}{\partial T_a}\right)^2\left(\frac{\overline{B_{T_a}}}{T_a}\right)^2} \tag{A4}$$

$$\frac{S_q}{q}=\sqrt{\left(\frac{\partial q}{\partial V}\right)^2\left(\frac{S_V}{V}\right)^2+\left(\frac{\partial q}{\partial T_a}\right)^2\left(\frac{\overline{S_{T_a}}}{T_a}\right)^2} \tag{A5}$$

$$\frac{U_{RSS,q}}{q}=\sqrt{\left(\frac{B_q}{q}\right)^2+t_{95}\left(\frac{S_q}{q}\right)^2} \tag{A6}$$

where, $\overline{B_{T_a}}$ and $\overline{S_{T_a}}$ are basis of the average temperature and precision index of the precision double bridge (Yokogawa, Type2752) for the temperature calibration, respectively. They can be expressed as follows:

$$\frac{\overline{B_{T_a}}}{T_a}=\sqrt{w_1^2\left(\frac{B_{V_T}}{V}\right)^2+w_2^2\left(\frac{B_R}{R}\right)^2} \tag{A7}$$

$$\frac{\overline{S_{T_a}}}{T_a}=\sqrt{w_1^2\left(\frac{S_{V_T}}{V}\right)^2+w_2^2\left(\frac{S_R}{R}\right)^2} \tag{A8}$$

where, w_1 and w_2 are weight coefficients as follows:

$$w_1=\frac{U_{RSS,V}}{U_{RSS,V}+U_{RSS,R}} \tag{A9}$$

$$w_2=1-w_1 \tag{A10}$$

where, $U_{RSS,V}$ and $U_{RSS,R}$ are uncertainties of the DC amplifier and the double bridge, respectively. They can be calculated by the following equations.

$$\frac{U_{RSS,V}}{V} = \sqrt{\left(\frac{B_{V_T}}{V}\right)^2 + \left(\frac{S_V}{V}\right)^2} \tag{A11}$$

$$\frac{U_{RSS,R}}{R} = \sqrt{\left(\frac{B_R}{R}\right)^2 + \left(\frac{S_R}{R}\right)^2} \tag{A12}$$

$$\frac{S_R}{R} = \sqrt{\frac{\sum_{k=1}^{N}(R_k - R_{LS,k})^2}{N-C}} \tag{A13}$$

where, B_R and S_R are the basis of the precision double bridge and precision index of the temperature calibration, respectively. N and C are a number of data and number of constant value for the least square (LS) method, respectively. Furthermore, the uncertainty of the heat transfer coefficient can be obtained by Eqs. (A14)- (A16).

$$\frac{B_h}{h} = \sqrt{\left(\frac{\partial h}{\partial q}\right)^2\left(\frac{B_q}{q}\right)^2 + \left(\frac{\partial h}{\partial \Delta T}\right)^2\left(\frac{B_{\Delta T}}{\Delta T}\right)^2} \tag{A14}$$

$$\frac{S_h}{h} = \sqrt{\left(\frac{\partial h}{\partial q}\right)^2\left(\frac{S_q}{q}\right)^2 + \left(\frac{\partial h}{\partial \Delta T}\right)^2\left(\frac{S_{\Delta T}}{\Delta T}\right)^2} \tag{A15}$$

$$\frac{U_{RSS,h}}{h} = \sqrt{\left(\frac{B_h}{h}\right)^2 + t_{95}\left(\frac{S_h}{h}\right)^2} \tag{A16}$$

where, $B_{\Delta T}$ and $S_{\Delta T}$ are the temperature difference between the surface temperature of the test heater and balk gas temperature and the precision index of the temperature difference, respectively. They can be expressed as follows.

$$\frac{B_{\Delta T}}{\Delta T} = \sqrt{\left(\frac{\overline{B_{T_a}}}{T_a}\right)^2 + \left(\frac{B_q}{q}\right)^2 + \left(\frac{B_{T_b}}{T_b}\right)^2} \tag{A17}$$

$$\frac{\delta_{\Delta T}}{\Delta T} = \sqrt{\left(\frac{\overline{\delta_{T_a}}}{T_a}\right)^2 + \left(\frac{\delta_q}{q}\right)^2 + \left(\frac{\delta_{T_b}}{T_b}\right)^2} \quad \text{(A18)}$$

References

[1] Q.S. Liu, M. Shibahara, and K. Fukuda, Transient heat transfer for forced convection flow of helium gas over a horizontal plate, *Experimental Heat Transfer*, Vol.21, pp.206-219, 2008.

[2] N. Tak, M.H. Kim, and W. J. Lee, Numerical Investigation of a Heat Transfer within the Prismatic Fuel Assembly of a Very High Temperature Reactor, *Annals of Nuclear Energy*, Vol. 35, pp.1892-1899, 2008.

[3] K. Sanokawa, Present and Future Development on High Temperature Gas Cooled Reactor in Japan, *Nuclear Industry* (in Japanese), Vol. 40-12, pp.13-18, 1994.

[4] K. Koyama and Y. Asako, Experimental Investigation on Heat Transfer Characteristics of a Gas-to Gas Counterflow Microchannel Heat Exchanger, *Experimental Heat Transfer*, Vol.23, pp.130-143, 2010.

[5] G. L. Morini, M. Lorenzini, S. Salvigni, and G. P. Celata, Experimental Analysis of Microconvective Heat Transfer in the Laminar and Transitional Regions, *Experimental Heat Transfer*, Vol.23, pp.73-93, 2010.

[6] L.X. Yang, A. Guo, and D. Liu, Experimental Investigation of Subcooled Vertical upward Flow Boiling in a Narrow Rectangular Channel, *Experimental Heat Transfer*, Vol.29, pp.221-243, 2016.

[7] M. Piasecka, The Use of Enhanced Surface in Flow Boiling Heat Transfer in a Rectangular Minichannel, *Experimental Heat Transfer*, Vol.27, pp.231-255, 2014.

[8] D. Deng, Q. Huang, W. Wan, W. Zhou, and Y. Lian, Experimental Study on Flow Boiling Pressure Drop and Flow Instabilities of Reentrant Micro-Channels, *Experimental Heat Transfer*, Vol.29, pp.811-832, 2016.

[9] Q.S. Liu and K. Fukuda, Transient Heat Transfer for Forced Convection Flow of Helium Gas, *JSME International Journal*, Series B, Vol.45-3, pp.559-564, 2002.

[10] Q.S. Liu, K. Fukuda, and Z. Zhang, Theoretical and experimental studies on transient heat transfer for forced convection flow of helium gas over a horizontal cylinder, *JSME International Journal*, Series B, Vol.49, No.2, pp.326-333, 2006.

[11] Z. Zhao, Q.S. Liu, and K. Fukuda, Experimental and numerical study on transient heat transfer for helium gas flowing over a flat plat containing an exponentially increasing heat source, *Mechanical Engineering Journal*, Vol.1, No.4, pp.1-13, 2014.

[12] K. Fukuda and Q. S. Liu, Steady and Transient Critical Heat Fluxes on a Horizontal Cylinder in a Pool of Freon-113, *International Journal of Transport Phenomena*, Vol.7, pp.71-83, 2005.

[13] Q.S. Liu, M. Shiotsu, and A. Sakurai, A Correlation for Forced Convection Film Boiling Heat Transfer from a Horizontal Cylinder, *Two-Phase Flow and Heat Transfer*, ed. by J. H. Kim et al., ASME Book, HTD-Vol. 197, pp. 101-110, 1992.

[14] M. Shibahara, Q.S. Liu, and K. Fukuda, Transient forced convection heat transfer for nitrogen gas flowing over plate heater with exponentially increasing heat input, International Journal of Heat and Mass Transfer, Vol. 95, pp. 405-415, 2016.

[15] ANSI/ASME PTC 19.1-1985, Measurement uncertainty, supplement on instruments and apparatus, part 1, 1987.

[16] Q.S. Liu and K. Fukuda, Transient Heat Transfer for Helium Gas Flowing over a Horizontal Cylinder with Exponentially Increasing Heat Input, *Proc. of the 11th International Conference on Nuclear Engineering* (ICONE-11), Paper No. ICONE11-36467, 2003.

[17] J.P. Holman, *Heat Transfer*, McGraw-Hill Book Company, Ninth Edition, Chap.5, pp.217, 2002.

Figure captions

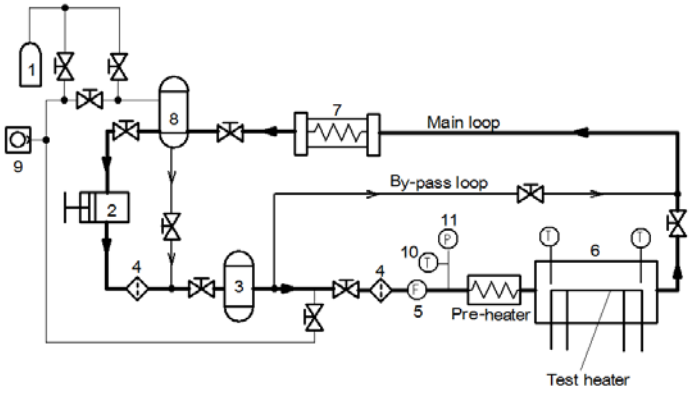

1.Gas cylinder 2.Compressor 3.Delivery surge tank 4.Filter
5.Turbine flow meter 6.Test section 7.Cooler 8.Suction surge tank
9.Rotary vacuum pump 10.Thermocouple 11.Pressure indicator

Figure 1. Schematic diagram of experimental apparatus.

Qiusheng LIU

Transient heat transfer for helium gas flowing over a horizontal cylinder in a narrow channel

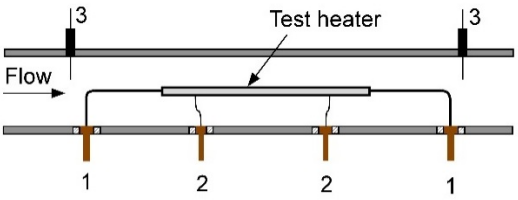

1. Current conductor 2. Potential conductor
3. Thermocouple

Figure 2. Test section.

Qiusheng LIU

Transient heat transfer for helium gas flowing over a horizontal cylinder in a narrow channel

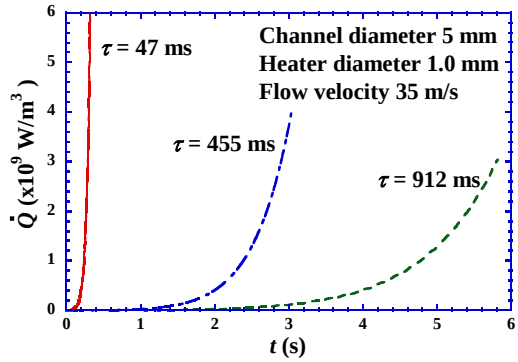

(a) Heat generation rate

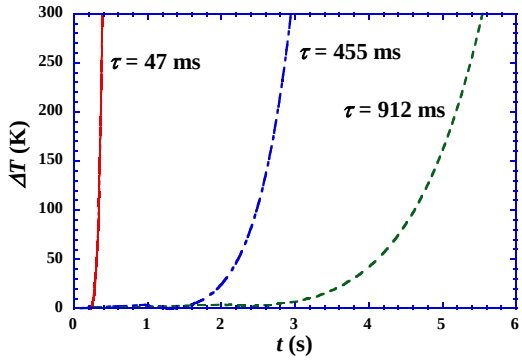

(b) Temperature difference

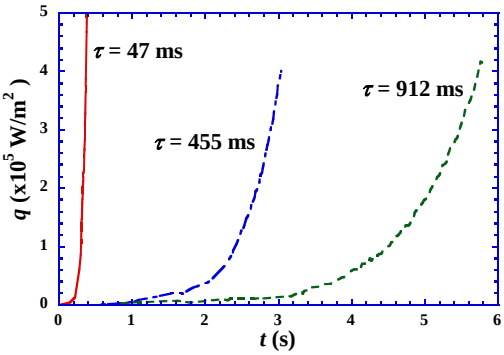

(c) Heat flux

Figure 3. The relation of $\dot{Q}$, ΔT, q with time.

Qiusheng LIU

Transient heat transfer for helium gas flowing over a horizontal cylinder in a narrow channel

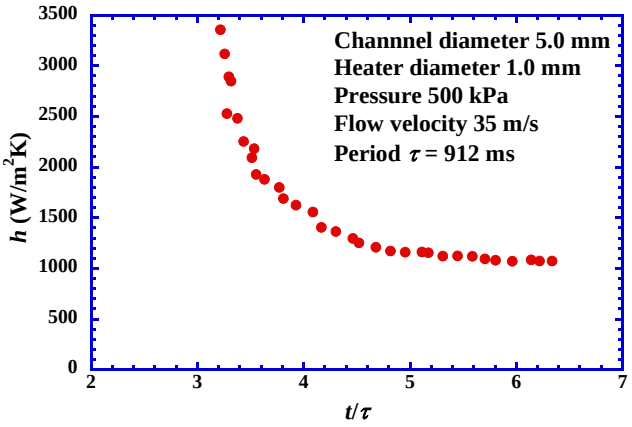

Figure 4. Heat transfer coefficient with the increase of time at periods of 912 ms.

Qiusheng LIU

Transient heat transfer for helium gas flowing over a horizontal cylinder in a narrow channel

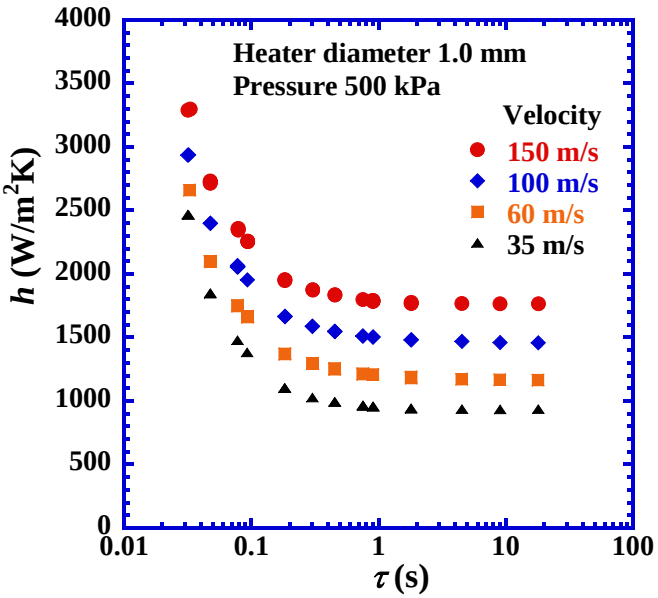

Figure 5. Heat transfer coefficients at various velocities and periods.

Qiusheng LIU

Transient heat transfer for helium gas flowing over a horizontal cylinder in a narrow channel

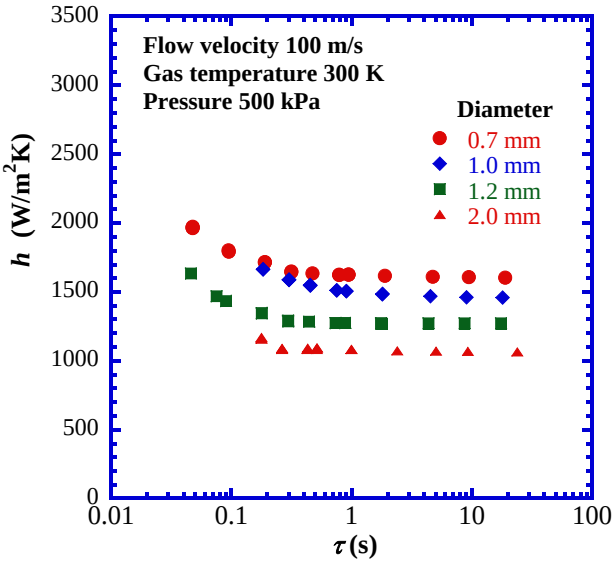

Figure 6. Heat transfer coefficients at various periods and cylinder diameters.

Qiusheng LIU

Transient heat transfer for helium gas flowing over a horizontal cylinder in a narrow channel

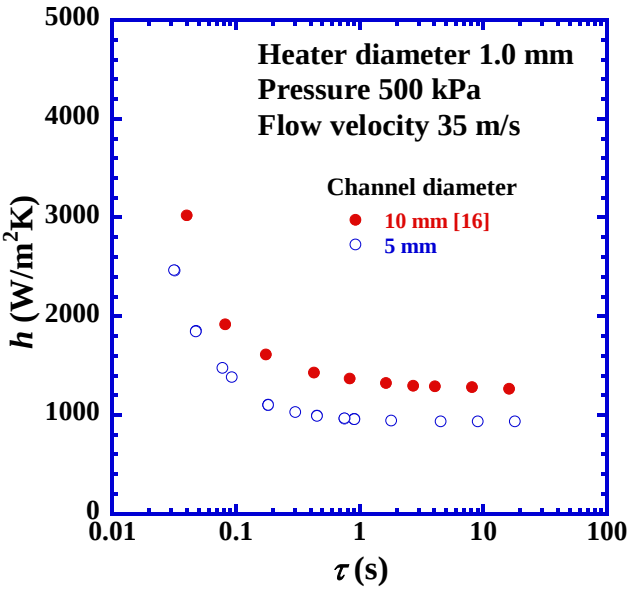

Figure 7. Heat transfer coefficient at different diameter of channel.

Qiusheng LIU

Transient heat transfer for helium gas flowing over a horizontal cylinder in a narrow channel

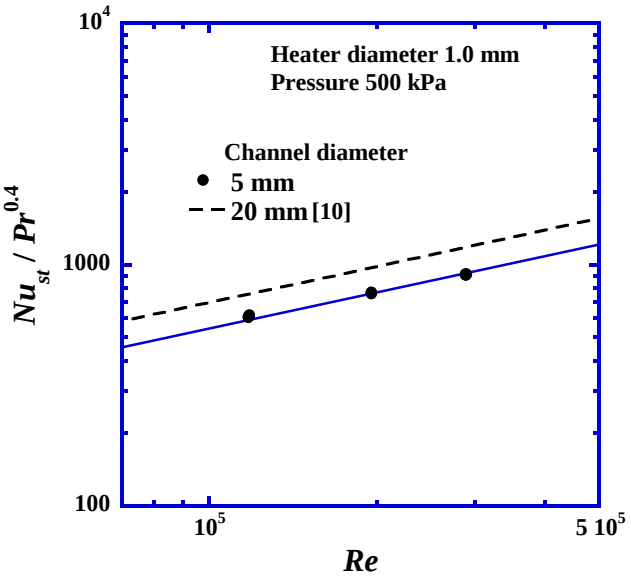

Figure 8. The relation of $Nu_{st}/Pr^{0.4}$ with Re at various channel diameters.

Qiusheng LIU

Transient heat transfer for helium gas flowing over a horizontal cylinder in a narrow channel

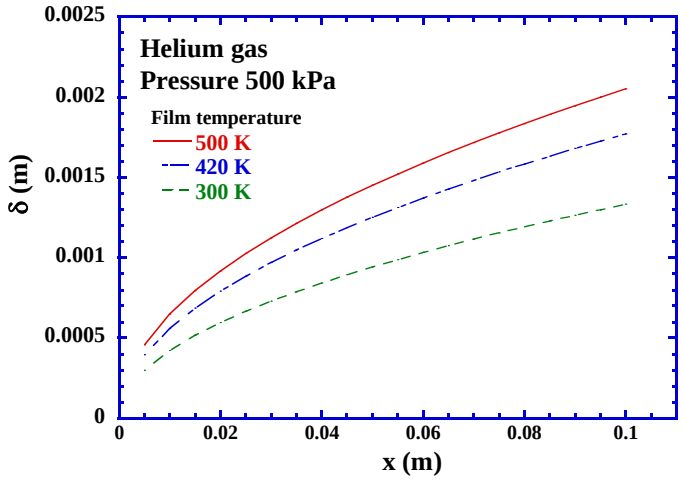

Figure 9. Thermal boundary layer thickness along the heater.

Qiusheng LIU

Transient heat transfer for helium gas flowing over a horizontal cylinder in a narrow channel

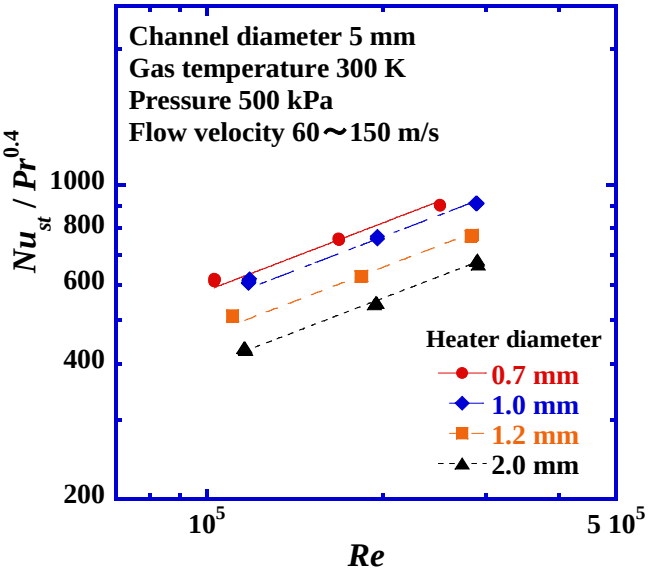

Figure 10. Nusselt number at various Reynolds numbers.

Qiusheng LIU

Transient heat transfer for helium gas flowing over a horizontal cylinder in a narrow channel

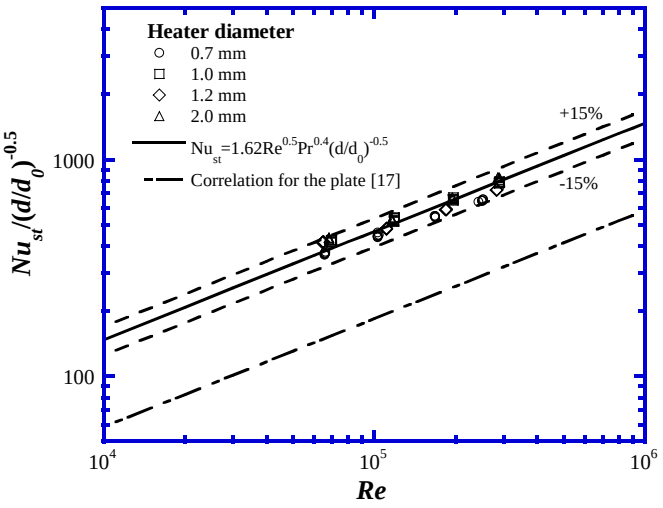

Figure 11. Comparison of the experimental data with the correlation for plate in laminar flow.

Qiusheng LIU

Transient heat transfer for helium gas flowing over a horizontal cylinder in a narrow channel

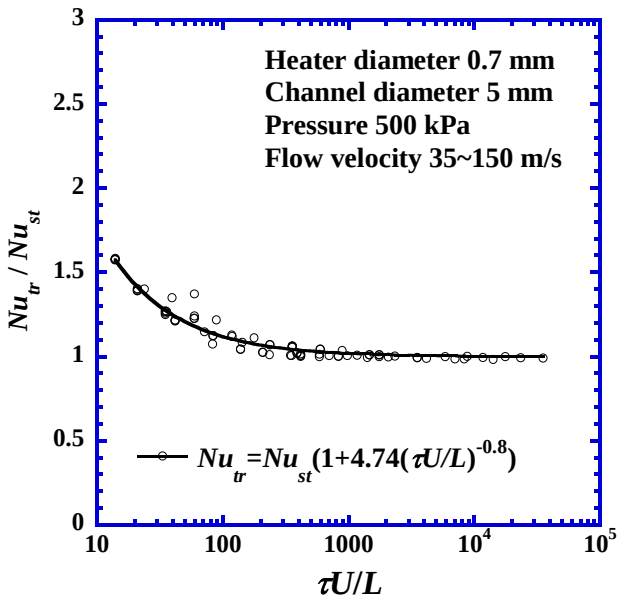

Figure 12. Transient Nusselt numbers at various velocities and periods.

Qiusheng LIU

Transient heat transfer for helium gas flowing over a horizontal cylinder in a narrow channel